J|A|C|S
ARTICLES
Published on Web 08/05/2006

Self-Assembled FePt Nanocrystals with Large Coercivity: Reduction of the fcc-to-$L1_0$ Ordering Temperature

Laudemir Carlos Varanda* and Miguel Jafelicci, Jr.

Contribution from the Laboratory of Magnetic Materials and Colloids, Department of Physical Chemistry, Institute of Chemistry, Universidade Estadual Paulista (UNESP), P.O. Box 355, 14801-970 Araraquara, São Paulo, Brazil

Received January 30, 2006; E-mail: lvaranda@posgrad.iq.unesp.br

Abstract: Herein we report the synthesis and properties of $Fe_{55}Pt_{45}$ nanoparticles, both monodisperse and self-assembled into hexagonal close-packed and cubic arrays of 4.0 ± 0.2 nm size in an $L1_0$ structure, obtained by a modified polyol process. The new synthetic route improved the control over the particle composition, thereby reducing the temperature required to convert from face-centered cubic (fcc) to face-centered tetragonal (fct) phase by some 30−50 °C without additives. Annealing at 550 °C for 30 min converts the self-assembled nanoparticles into ferromagnetic nanocrystals with large coercivity, H_C = 11.1 kOe. Reducing the fcc-to-fct ($L1_0$) ordering temperature avoided particle coalescence and decreased the loss in particle positional order without compromising the magnetic properties, as is generally observed when additives are used.

Introduction

Structural, magnetic, electronic, and catalytic properties of many materials are strongly size-dependent at the nanometer scale, and the preparation of high-quality nanocrystals of desired size is of great fundamental and technological interest.[1−3] The synthesis of metal colloids has been studied for more than a century, yet the number of preparations yielding a size series of monodisperse metal nanocrystals is surprisingly small.[1,4,5] Control of nanocrystal size and composition is key in the formation of two- and three-dimensional self-assembled structures where the individual nanocrystals play the role of building-blocks − artificial atoms in the next level of material hierarchy.[1,3,6,7] Moreover, in the past decades, magnetic recording technology has made tremendous gains in data storage density, partially by scaling down the grain size of thin-film media.[2,8,9] In this direction, one of the Chemistry Highlights of 2000 was reported bySun and co-workers[7] at IBM, regarding the synthesis, self-assembly, and magnetic recording performance of FePt nanoparticles.[10,11]

However, before the application of self-assembled FePt nanocrystals in high-density magnetic data storage can be realized, some problems must be solved. Perhaps one of the most challenging problems is how to avoid particle coalescence/sintering and positional order loss after annealing to promote the phase transformation from face-centered cubic (fcc) to face-centered tetragonal (fct, $L1_0$).[8,10−13] As-synthesized FePt nanoparticles have an fcc structure and are superparamagnetic at room temperature. Annealing above 500 °C converts the superparamagnetic nanoparticles into ferromagnetic fct phase nanocrystals, having high magnetocrystalline anisotropy. In general, for complete phase transformation, the particles must be heated to 580 °C.[3] However, annealing at temperatures above 550 °C leads to considerable particle coalescence and positional order loss. Thus, it is highly desirable to lower the temperature required for fcc-to-fct ($L1_0$) phase transformation, at least to below temperatures where the particles coalesce.

The literature has reported decreases in the temperature required for fcc-to-fct phase transformation resulting from addition of copper or silver into sputtered CoPt or FePt films,[14−16] suggesting that additives can decrease the temperature of the phase transformation for nanoparticulate materials. Quite recently, Kang et al.[10] observed that addition of Ag reduced the annealing temperature required to promote the tetragonal phase formation for FePt nanoparticles. The effect of the additive is not obvious, and X-ray diffraction data showed that some metallic silver segregation seems to occur during annealing. This

(1) Murray, C. B.; Kagan, C. R.; Bawendi, M. G. *Annu. Rev. Mater. Sci.* **2000**, *30*, 545−610.
(2) Varanda, L. C.; Jafelicci, M., Jr.; Tartaj, P.; O'Grady, K.; Gonzalez-Carreno, T.; Morales, M. P.; Muñoz, T.; Serna, C. J. *J. Appl. Phys.* **2002**, *92*, 2079−2085.
(3) Sun, S.; Fullerton, E. E.; Weller, D.; Murray, C. B. *IEEE Trans. Magn.* **2001**, *37*, 1239−1243.
(4) Shevchenko, E. V.; Talapin, D. V.; Schnablegger, H.; Kornowski, A.; Festin, O.; Svedlindh, P.; Haase, M.; Weller, H. *J. Am. Chem. Soc.* **2003**, *125*, 9090−9101.
(5) Leslie-Pelecky, D. L.; Rieke, R. D. *Chem. Mater.* **1996**, *8*, 1770−1783.
(6) Rogach, A. L.; Talapin, D. V.; Shevchenko, E. V.; Kornowski, A.; Haase, M.; Weller, H. *Adv. Funct. Mater.* **2002**, *12*, 653−664.
(7) Sun, S.; Murray, C. B.; Weller, D.; Folks, L.; Moser, A. *Science* **2000**, *287*, 1989−1992.
(8) Chen, M.; Nikles, D. E. *Nano Lett.* **2002**, *2*, 211−214.
(9) Varanda, L. C.; Morales, M. P.; Goya, G. F.; Imaizumi, M.; Serna, C. J.; Jafelicci, M. *Mater. Sci. Eng. B−Solid State* **2004**, *112*, 188−193.
(10) Kang, S.; Harrell, J. W.; Nikles, D. E. *Nano Lett.* **2002**, *2*, 1033−1036.
(11) Borman, S. *Chem. Eng. News* **2000**, *78* (51), 24−31.
(12) Klemmer, T. J.; Shukla, N.; Liu, C.; Wu, X. W.; Svedberg, E. B.; Mryasov, O.; Chantrell, R. W.; Weller, D. *Appl. Phys. Lett.* **2002**, *81*, 2220−2222.
(13) Dai, Z. R.; Sun, S.; Wang, Z. L. *Nano Lett.* **2001**, *1*, 443−447.
(14) Maeda, T.; Kai, T.; Kikitsu, A.; Nagase, T.; Akiyama, J. *Appl. Phys. Lett.* **2002**, *80*, 2147−2149.
(15) Maeda, T.; Kikitsu, A.; Kai, T.; Nagase, T.; Aikawa, H.; Akiyama, J. *IEEE Trans. Magn.* **2002**, *38*, 2796−2798.
(16) Kitakami, O.; Shimada, Y.; Oikawa, K.; Daimon, H.; Fukamichi, K. *Appl. Phys. Lett.* **2001**, *78*, 1104−1106.

10.1021/ja060711i CCC: $33.50

segregation could lead to vacancy formation in the FePt lattice, inducing an increase in the mobility of the Fe and Pt atoms, enhancing the kinetics of phase transformation. Although reduction of the annealing temperature was observed when using additives, the magnetic properties, mainly the coercivity, of the completely transformed final product in a tetragonal phase were much lower than those observed for pure $L1_0$ FePt nanoparticles.

In this work, we report the synthesis of pure $Fe_{55}Pt_{45}$ ferromagnetic nanocrystals in an $L1_0$ structure by a modified polyol process and a significant decrease in the temperature of the tetragonal phase formation without addition of additives.

Experimental Section

Synthesis of FePt Nanoparticles. We have modified the synthetic polyol process reported by Sun et al. to prepare Fe_xPt_{100-x} nanoparticles. Our synthetic experiments were carried out using a standard airless procedure and commercially available reagents without further purifications. Typical $Fe_{55}Pt_{45}$ preparation was carried out as follows: in a three-necked round-bottom flask under nitrogen atmosphere, platinum acetylacetonate ($Pt(acac)_2$, 0.5 mmol) and 1,2-hexadecanediol (1.5 mmol) were mixed in 20 mL of dioctyl ether and heated to 100 °C. To this solution were added via syringe oleic acid (0.5 mmol), oleylamine (0.5 mmol), and a quantitative amount of 0.09 mol L^{-1} iron(III) acetylacetonate, preheated at 70 °C in 2-propanol ($Fe(acac)_3$, 0.61 mmol, 6.8 mL) solution. The resulting mixture was heated to reflux (~298 °C) and allowed to reflux for 30 min, giving a black dispersion. The heat source was removed, and the dispersion was allowed to cool to room temperature. Ethanol (~40 mL) was then added to separate the nanoparticles, and the particles were isolated by centrifuging. The particles were redispersed in hexane, precipitated with ethanol, and isolated by centrifugation three times. Although the redispersion and separation procedures purified the particles, we did not analyze the wash. Finally, purified nanoparticles were dried at room temperature under vacuum. The $Fe(acac)_3$ 2-propanolic solution volume can be varied in order to obtain different nanoparticle compositions. For example, $Fe_{50}Pt_{50}$ was prepared by adjusting the Pt/Fe ratio using 0.5 mmol of $Pt(acac)_2$ and 0.5 mmol (5.5 mL) of $Fe(acac)_3$ and following the experimental procedure described above.

Synthesis of Nanoparticle Assemblies. Self-assembled materials were obtained by redispersing the nanoparticles in a 50/50 mixture of hexane and octane (for example, 2 mg of particle in 1 mL of solvent) containing 0.1 mL of a 50/50 mixture of oleic acid and oleylamine. The resulting dispersion was dropped onto a silica slide substrate for structural and magnetic properties analysis or onto a carbon-coated copper grid for transmission electron microscopy (TEM) analysis. The solvent was slowly evaporated at room temperature. As-deposited thin films were then transferred into a tube furnace (Thermolyne F79400) and annealed for 30 min with nitrogen flowing, containing 5% hydrogen, at temperatures ranging from 400 to 700 °C. The samples were taken out of the furnace and cooled to room temperature in a nitrogen atmosphere, giving smooth and reflective films which can be handled and stored under ambient conditions.

Characterization of FePt Nanoparticles and Nanoparticle Assemblies. Morphology, particle size, and size distributions were investigated by TEM using a Philips CM200 microscope operating at 200 kV. FePt nanoparticles and nanoparticle assemblies were made by dropping dilute particle dispersions onto a carbon-coated copper grid, and the solvent was slowly evaporated at room temperature. In addition, the single-crystal character and the orientation of the crystallographic axes of the FePt nanoparticles were studied by high-resolution TEM (HRTEM). The average particle size diameters (d) and their standard deviation (σ) were determined statistically in order to obtain the degree of polydispersity (δ) of the systems. The chemical composition of the nanoparticles was determined by both inductively coupled plasma (ICP) atomic emission spectroscopy, performed in a Perkin-Elmer Plasma 40 spectrometer, and energy-dispersive X-ray analysis (EDS), performed on a JEOL-JSM T330A scanning electron microscope equipped with an EDS probe. Nanoparticle structure was determined by X-ray powder diffraction (XRD) on a Rigaku RINT2000 diffractometer using Cu Kα radiation ($\lambda = 1.5418$ Å). The ~0.5-μm-thick samples were deposited onto a microslide substrate (1×1 cm^2). The average crystallite size was estimated by Scherrer analysis[17] from the full-width at half-maximum (fwhm) of the (111) reflection. Magnetic studies were carried out using a commercial vibrating sample magnetometer (VSM) with fields up to 7 T at room temperature. Measurements were done on thick nanoparticle assemblies (>100 nm) on a silica microslide (0.5×0.5 cm^2) and loaded perpendicular and parallel to the magnetic field.

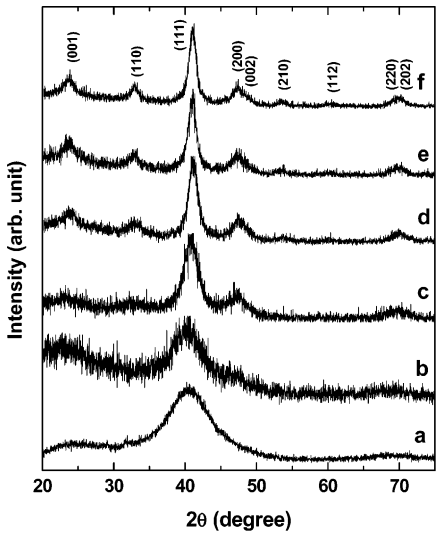

Figure 1. XRD patterns of the self-assembled $Fe_{55}Pt_{45}$ nanoparticles: (a) as-synthesized and a series of similar assemblies annealed under nitrogen/hydrogen (5%) flowing for 30 min at temperatures of (b) 400, (c) 500, (d) 550, (e) 580, and (f) 600 °C.

Results and Discussion

The results of nanoparticle composition analysis showed that control over the composition was more efficient than that obtained when iron pentacarbonyl was used as the iron source.[18] Results from ICP and EDS composition analysis were in good agreement and showed that the composition of either a single nanoparticle or a group of FePt nanoparticles determined by EDS matches well with the composition of the bulk FePt samples obtained by ICP analysis. Moreover, the best composition control was achieved by the modified experimental procedure yielding the $Fe_{55}Pt_{45}$ stable phase, which is the optimized composition for the highest coercive FePt nanoparticle materials.[3,18]

Changes in the internal particle crystalline structure upon annealing were studied by X-ray diffraction (XRD). Figure 1 shows a series of XRD patterns for ~0.5-μm-thick $Fe_{55}Pt_{45}$ assemblies as a function of annealing temperature at a constant annealing time of 30 min. As-synthesized (Figure 1a) nanoparticles present the chemically disordered fcc structure. At an annealing temperature of 400 °C, fcc is the only phase observed in the XRD patterns. Careful examination of curve c in Figure 1 shows that very weak (001) and (110) reflections for the chemically ordered fct phase of FePt appeared after heat

(17) Cullity, B. C. In *Elements of X-ray diffraction*; Addison-Wesley Publishing Co., Inc.: London, 1978.
(18) Varanda, L. C.; Imaizumi, M.; Jafelicci, M., Jr. Monodisperse $Fe_XPt_{(1-X)}$ nanoparticle materials with high chemical composition control by a modified polyol process. *Adv. Funct. Mater.* **2006**, submitted.

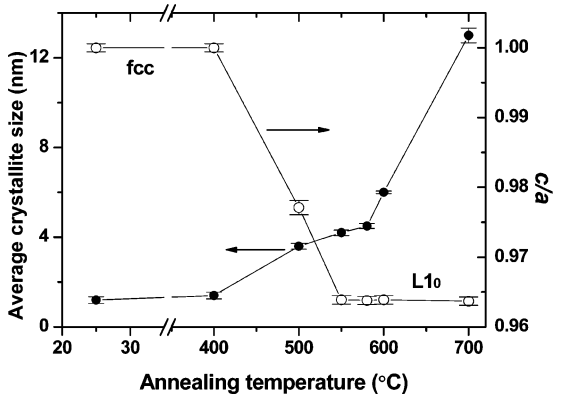

Figure 2. Effects of annealing temperature on the degree of transformation to the tetragonal phase, quantified by the quotient c/a (open symbols), and on the average crystallite size (filled symbols) for $Fe_{55}Pt_{45}$ sample annealed for 30 min.

treatment at 500 °C. Thus, at annealing temperatures below 500 °C, the fcc structure is the only phase observed, and at 500 °C, partial chemical ordering takes place. X-ray diffraction patterns of the samples annealed above 550 °C match the fct phase of FePt. Therefore, annealing causes the Fe and Pt atoms to rearrange into the long-range chemically ordered fct structure, as indicated by (111) reflection shifts and the evolution of the (001) and (110) reflections observed for samples annealed at 550 °C and above (Figure 1d−f).

Atomic rearrangements lead to the iron atomic plane being intercalated with the platinum atomic planes in the *c* direction of the platinum lattice in the fct structure. It results from the effective lattice contraction in the *c* direction due to the difference in the atomic radii, Fe = 1.24 Å and Pt = 1.38 Å. As a consequence of this tetragonal distortion, the (111) fcc phase reflection is displaced from 40.2° (2θ) to 41.1° (2θ) in the fct phase, as observed in Figure 1. XRD also showed that annealing at high temperatures, for example ≥580 °C, results in small pattern changes. However, the average crystallite size, estimated by the Scherrer equation[17] using the (111) reflection of the FePt X-ray diffraction results, shows a significant increase of this parameter for samples annealed at temperatures higher than 580 °C, in agreement with the report by Dai et al. (Figure 2).[13] Accurate studies by Thomson et al.[19] resulted in a model of FePt nanoparticles in which the magnetic and structural properties can only be explained by considering the as-synthesized nanoparticles as presenting a complex core/shell structure. In their model, a metallic FePt fcc core is coated with an oxide shell containing highly superparamagnetic clusters of atoms. Thus, during annealing, the Fe-containing shell of superparamagnetic materials is continuously incorporated into the FePt metallic core. This model supports our results indicating a smaller crystallite size (∼2.0 nm) compared to the average particle size (∼4.0 nm) determined by TEM analysis. These results can be understood from XRD data, which are analyzed by determining the width of the peaks from well-defined (111) crystallographic planes, corresponding to the metallic FePt core. The completely disordered Fe-containing shell of superparamagnetic materials does not contribute to the XRD results. Until an annealing temperature of 400 °C, this incorporation is small because the diffusion of the atoms is slow and the crystallite size increases slightly,[19] as shown in Figure 2. Above 400 °C, the crystallite size corresponding to the metallic FePt core increases quickly due to the fast diffusion of the atoms. Around 550−600 °C, crystallite size and particle diameter present similar values, indicating that practically all the shell materials were incorporated into the core; thus, slight increases in crystallite size can be observed (Figure 2). Crystallite size increases greatly at annealing temperatures beyond 600 °C because FePt nanocrystals coalesce to form larger grains.[13]

Figure 2 also presents the tetragonal ordering, or degree of transformation to the tetragonal phase, quantified by the ratio c/a, where a and c are the unit cell parameters determined by XRD analysis.[8] For the fcc phases, $a = c$ and $c/a = 1$. Thus, the fcc-to-fct transformation induces a decrease in the ratio c/a to a limiting value. For FePt fct ($L1_0$) phase, $a = 3.8525$ Å and $c = 3.7133$ Å, giving a ratio $c/a = 0.9636$. In the study of the annealing temperature effects on the tetragonal ordering (Figure 2), at an annealing temperature around 500 °C, only partially chemically ordered $L1_0$ phase is observed, as indicated by the ratio $c/a = 0.9771$, as also observed from the XRD patterns (Figure 1c). Structural chemical ordering can be increased by annealing at high temperature (Figures 1 and 2) or increasing the annealing time (data not shown). Thus, according to Figure 2, the complete fcc-to-fct transformation was achieved at 550 °C, a temperature 30−50 °C lower than that reported as the optimized temperature to allow the pure FePt phase transformation.[7] According to the XRD patterns (Figure 1), using $Fe(acac)_3$, the fcc (111) reflection is very intense and the reflection corresponding to fcc (200) is not observed, which suggests that particles are essentially formed in (111) planes,[20,21] in agreement with the *magic number* used in the nanosized materials theory for particles smaller than 2.0 nm.[10,22,23] The absence of the (200) reflection implies the existence of structural defects. In the solid state, the rearrangement of atoms, besides energy, depends mainly on their mobility in the lattice. Structural defects favor the atoms' mobility in the lattice, similar to what was reported by Kang et al.,[10] who synthesized Ag-doped FePt nanoparticles, in which Ag segregation during annealing generates structural defects (vacancies) and favors the platinum and iron atoms' mobility, providing decreases in the annealing temperature. In our case, the defects seem to be less pronounced and the temperature decrease is smaller than that observed when additives were used.

Transmission electron microscopy was performed for samples annealed at 550 °C for 30 min. TEM images (Figure 3) reveal that the nanoparticle systems are monodisperse, with average particle diameter of 4.0 ± 0.2 nm and degree of polydispersity[24] $\sigma \leq 5\%$. Nanoparticle samples readily self-assembled into two- or three-dimensional superlattices. Figure 3a,b shows nanoparticles assembled into a two-dimensional (2D) hexagonal close-packed array of $Fe_{55}Pt_{45}$ sample, with a nearest-neighbor spacing of ∼1.5 nm maintained by oleic acid and oleylamine capping group effects. In fact, annealing at 550 °C does not result in

(19) Thomson, T.; Toney, M. F.; Raoux, S.; Lee, S. L.; Sun, S.; Murray, C. B.; Terris, B. D. *J. Appl.* Phys. **2004**, *96*, 1197−1201.
(20) Nandwana, V.; Elkins, K. E.; Liu, J. P. *Nanotechnology* **2005**, *16*, 2823−2826.
(21) Iwaki, T.; Kakihara, Y.; Toda, T.; Abdullah, M.; Okuyama, K. *J. Appl. Phys.* **2003**, *94*, 6807−6811.
(22) Boyen, H. G.; Kastle, G.; Weigl, F.; Koslowski, B.; Dietrich, C.; Ziemann, P.; Spatz, J. P.; Riethmuller, S.; Hartmann, C.; Moller, M.; Schmid, G.; Garnier, M. G.; Oelhafen, P. *Science* **2002**, *297*, 1533−1536.
(23) Watzky, M. A.; Finke, R. G. *J. Am. Chem. Soc.* **1997**, *119*, 10382−10400.
(24) Hunter, R. J. *Foundations of colloid science*; Clarendon Press: Oxford, 1989.

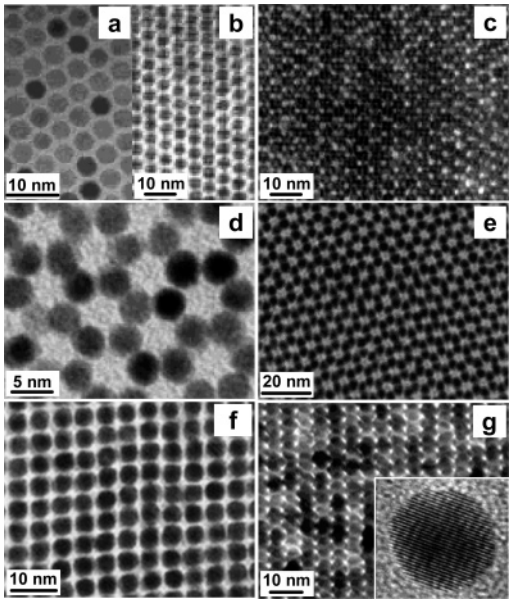

Figure 3. TEM images of self-assembled $Fe_{55}Pt_{45}$ annealed at 550 °C for 30 min into hexagonal arrays (oleic acid/oleylamine as spacers): 2D close-packed at higher (a) and lower (b) magnification; 3D close-packed (c); and honeycomb type at higher (d) and lower (e) magnification. Nanoparticles assembled into cubic arrays (hexanoic acid/hexylamine as spacers): 2D (f) and 3D (g). The inset in (g) presents the HRTEM of individual nanocrystal, showing the texture along the (111) planes.

the complete loss of stabilizing ligands, but rather they are converted into a carbonaceous coating around each particle. Moreover, the three-dimensional (3D) hexagonal close-packed array (Figure 3c) was observed in the multilayer region and can be obtained by using a more highly concentrated dispersion (5 mg of particle in 1 mL of solvent). The structure of the hexagonal array can be also tuned by the particle concentration in the assembled thin film. When a highly concentrated dispersion (2 mg of particle in 1 mL of solvent) was used, nanoparticles self-assembled into an ABC hexagonal close-packed array, as shown in Figure 3a,b. If a lower concentration dispersion ($\leq$1 mg of particle in 1 mL of solvent) was used, the assembly exhibited a honeycomb-type array (Figure 3d,e), consistent with the AB stacking of the particles.

In addition, room-temperature ligand exchange of the long-chain capping groups, oleic acid and oleylamine — or, for shorter hexyl groups, hexanoic acid and hexylamine — was performed to allow the interparticle distance to be adjusted. Dried nanoparticles in a vacuum oven were re-dispersed in ethanol using an ultrasonic bath for 10 min and separated by centrifuging. This procedure was repeated twice in order to promote the nanoparticle surface cleaning. After that, nanoparticles were re-dispersed in hexane containing hexanoic acid and hexylamine, and the suspension was maintained under stirring for 30 min. Particles were then separated by ethanol addition, centrifuged, and dried in a vacuum oven at room temperature. As mentioned before, the self-assembly procedure was modified by changing the capping groups mixture to hexanoic acid and hexylamine.

Ligand exchange yielded a cubic packing in 2D (Figure 3f) and 3D (Figure 3g) arrays with $\sim$1 nm interparticle spacing.[7,25] A transformation from hexagonal to cubic packing has been observed in monodisperse nanoparticle assemblies upon changing the capping groups.[7] It is important to emphasize that long-range ordering can be observed in all assembled samples and that annealing at 550 °C does not change the average particle size or promote coalescence in the self-assembled materials, indicating that the reduction in the temperature of fcc-to-fct transformation is effective and entirely preserves the assembly. The inset in Figure 3g shows the high-resolution TEM (HRTEM), indicating a lattice spacing of 2.20 Å, characteristic of (111) planes. The texture presented in the HRTEM implies high structural homogeneity of the fct phase and indicates the formation of nanocrystals after annealing, in agreement with the results presented in Figure 2.

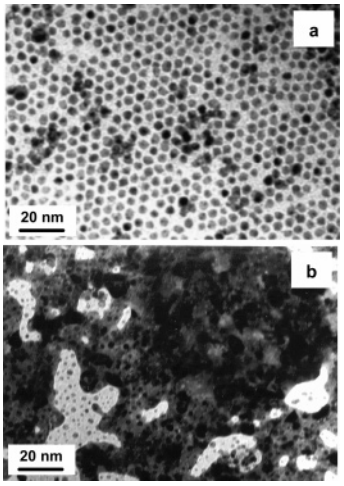

Figure 4. TEM images of self-assembled $Fe_{55}Pt_{45}$ annealed for 30 min at 600 (a) and 700 °C (b).

The TEM image of the sample annealed at 600 °C for 30 min (Figure 4a) revealed many coalesced regions, while annealing at 700 °C promoted an extensive coalescence process (Figure 4b), and the sample feature was similar to that observed in sintered metallic alloys. These results are in agreement with the average crystallite size greatly increasing after annealing at 600 °C (Figure 2) and with the recent work by Dai et al. that reported coalescence of FePt nanocrystals to form larger grains when annealed at temperatures above 600 °C.[13] Figure 5 shows a comparison of the in-plane and out-of-plane hysteresis loops of the self-assembled $Fe_{55}Pt_{45}$, annealed at 550 °C for 30 min, in cubic and hexagonal close-packed arrays, measured in a conventional SQUID at room temperature. As-prepared FePt nanoparticles presented superparamagnetic behavior (coercivity, $H_C = 0$ Oe), consistent with the low magnetocrystalline anisotropy of the fcc particle structure. According to the XRD results and magnetic measurements data, annealing at 550 °C converts the particle structure from the chemically disordered fcc phase to the chemically ordered fct phase and transforms the superparamagnetic nanoparticles into an assembly of ferromagnetic nanocrystals with larger coercivity, in agreement with the high magnetocrystalline anisotropy of the $L1_0$ phase.

The influence of the structural arrays on the magnetic properties can also be observed in Figure 5. For both in-plane ($H_{C,||}$) and out-of-plane ($H_{C,\perp}$) coercivity values, the hexagonal close-packed array ($H_{C,||} = 5.8$ kOe and $H_{C,\perp} = 11.1$ kOe) showed higher coercivity values than those obtained for the cubic array ($H_{C,||} = 4.9$ kOe and $H_{C,\perp} = 8.0$ kOe). This difference between coercivities of the hexagonal and cubic arrays can be explained by an increase in the interparticle

(25) Verdes, C.; Ahner, J.; Jones, P. M.; Shukla, N.; Chantrell, R. W.; Weller, D. *Appl. Phys. Lett.* **2005**, *86*, 263106 (1−3).

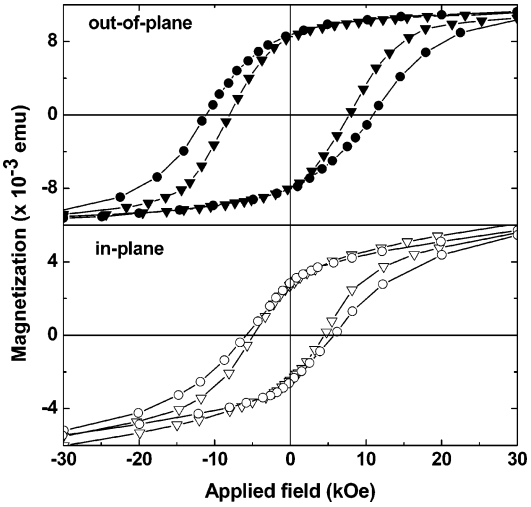

Figure 5. Room-temperature in-plane (open symbols) and out-of-plane (filled symbols) hysteresis loops of self-assembled $Fe_{55}Pt_{45}$ ferromagnetic nanocrystals annealed at 550 °C for 30 min into hexagonal close-packed (circles) and cubic (triangles) arrays.

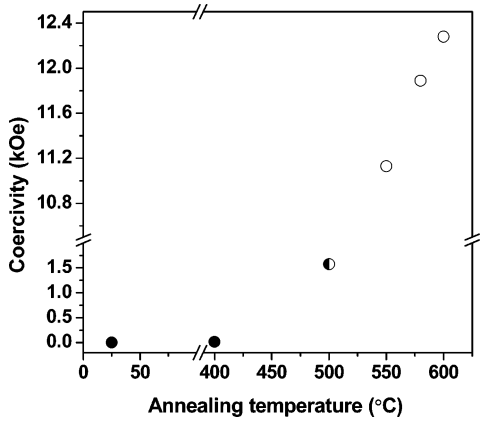

Figure 6. Room-temperature out-of-plane coercivity values as a function of annealing temperature for self-assembled $Fe_{55}Pt_{45}$ ferromagnetic nanocrystals in a hexagonal close-packed array and annealed for 30 min, indicating the face-centered cubic phase (filled symbols), partial face-centered cubic to face-centered tetragonal phase transformation (semi-filled symbol), and completely converted face-centered tetragonal phase (open symbols).

interactions (coupling) due to decreased particle spacing in the cubic structure ordering. Also, the difference between the in-plane and out-of-plane coercivity values and the observed hysteresis behavior indicate a non-random orientation or, at least, partial orientation of the easy axes of individual $Fe_{55}Pt_{45}$ ferromagnetic nanoparticle assemblies. However, the larger out-of-plane coercivity value observed for $Fe_{55}Pt_{45}$ nanocrystals is still much smaller than that expected of the FePt bulk. This result suggests that random magnetic orientation still remains and interparticle interactions can be present. Moreover, the shape of the magnetic hysteresis loops reveals the absence of any inflection in the magnetization near $H = 0$, which is characteristic of an isotropic distribution of particles with high anisotropy. Figure 6 shows the out-of-plane coercivity as a function of annealing temperature for $Fe_{55}Pt_{45}$ ferromagnetic nanocrystals assembled into hexagonal close-packed arrays, measured at room temperature. Consistent with the XRD data, the coercivity values increase dramatically with annealing temperature, showing the transition from superparamagnetic to ferromagnetic behavior. As mentioned before, as-synthesized nanocrystals and those annealed at 400 °C appear nearly superparamagnetic at room temperature. The sample annealed at 500 °C shows a coercivity value of ~1500 Oe, consistent with a minority fraction of the particles having sufficient anisotropy to be ferromagnetically ordered at room temperature.[3]

Annealing at high temperature rapidly increases the coercivity values ($H_C = 11.1$ kOe at room temperature for sample annealed at 550 °C), in agreement with the XRD results and the trends shown in Figure 2, due to complete fct phase transformation. Also consistent with the results presented in Figure 2, the coercivity continues to increase as the annealing temperature is increased above 550 °C because of particle growth due to coalescence, as indicated by the TEM images (Figure 4). We also assign the coercivity increase shown in Figure 6, even above 550 °C, to the increase in the fraction of $L1_0$ phase in the particle's metallic core, according to Thomson's model. This magnetic behavior was expected until the maximum shell incorporation that seems to occur at temperatures above 800 °C.[25] It is important to emphasize that magnetic properties are also strongly dependent on the nanoparticles' composition[3,18] and that improvement in the coercivity values, as well as reduction in the annealing temperature, is a consequence of enhancing the control over the composition by using the modified polyol process, which leads to $Fe_{55}Pt_{45}$ phase stabilization.

Conclusions

Magnetic $L1_0$ alloys are characterized by very large magnetic anisotropies that are definitively compatible with the future generation of ultra-high-density data storage. Thus, if self-assembled thin films of tetragonal FePt nanocrystals are to be used, a means of transforming the nanoparticles into the tetragonal phase, while maintaining the particle size and the high degree of particle position order, must be found. We believe that the results reported here are a very important step toward that goal. The annealing temperature of 550 °C required to convert the fcc phase to fct phase was some 30−50 °C lower than that normally reported for FePt nanoparticles. This temperature decrease was obtained without use of additives that promote the temperature decreasing but at the cost of a decrease in the magnetic properties. The enhancement in the control over nanoparticle composition obtained with the modified polyol process seems to be the key to improving the required properties that make assembled FePt nanocrystals useful. This enhancement has allowed for the preparation of $Fe_{55}Pt_{45}$ and seems also to promote structural defects in the fcc phase, improving the mobility of platinum and iron atoms and yielding a reduction in the annealing temperature without the use of additives. Two immediate benefits of lowering the transformation temperature were noted: significant improvements in the maintenance of the nanoparticle position order and avoidance of coalescence. Furthermore, although cubic arrays are preferred for use in magnetic storage, the results reported here show that interparticle interactions (coupling) in this structure organization are larger than those observed in hexagonal close-packed arrays. This interparticle coupling promotes a slight decrease in the out-of-plane coercivity, from $H_{C,\perp} = 11.1$ kOe for hexagonal arrays to $H_{C,\perp} = 8.0$ kOe for cubic arrays.

Acknowledgment. This work was supported by the Brazilian agency Fundação de Amparo à Pesquisa do Estado de São Paulo (FAPESP), award nos. 04/06762-0 and 04/02407-1.

JA060711I